Convection Heat Transfer Due to Protruded Heat Sources in an Enclosure

L. Chen*
Chongqing University, Sichuan, China
and
M. Keyhani† and D. R. Pitts‡
University of Tennessee-Knoxville, Knoxville, Tennessee 37916

An experimental study of convective heat transfer in a rectangular enclosure with 10 protruding heaters from one vertical wall has been performed. The top surface of the enclosure was a heat exchanger maintained isothermally as the heat sink. All of the other surfaces, except the heater locations, were unheated. Distilled water and ethylene glycol were used as working fluids. The heaters were numbered sequentially from bottom to top, and experimental results show that the bottom heater (heater 1), except for high Rayleigh number runs, has the highest heat transfer coefficient. The heat transfer coefficients at heaters 7, 8, and 9 are nearly the same and present the lowest values among the heaters. It is shown that the heat transfer coefficient decreases with increasing vertical position up to heater 7. At high Rayleigh numbers, the top heater (10) exhibited the highest heat transfer coefficients. Flow visualization experiments were also performed. Photographs of the flow patterns under several power inputs with glycol as the working fluid indicate the existence of a core flow within the enclosure and a recirculating cell in the gap between heaters. These pictures provide a clear basis for improved understanding of the flow mechanisms in an enclosure of the type used in the present study.

Nomenclature

A_h = surface area of a heated section, m^2
c = isobaric specific heat, J/kgK
g = acceleration due to gravity, m/s^2
H = height of the enclosure, m
h = local heat transfer coefficient, W/m^2K
k = thermal conductivity of the fluid, W/mK
L_1 = heater width, m
L_2 = gap between heaters, m
L_3 = protruding height, m
N = heater row number (starting from the bottom)
Nu = Nusselt number, h [length scale]$/k$
Pr = Prandtl number, ν/α
q = convective heat flux per heater section, W/m^2
Q = power input per heated section, W
Q_L = heat loss per heater to the environment, W
Q_{sc} = substrate conduction heat transfer per heated section (convected energy from unheated sections to the working fluid), W
Ra^* = modified Rayleigh number, $g\beta q$ [length scale]$^4/k\nu\alpha$
T = temperature, K
T_{core} = fluid temperature at the midhorizontal gap location, K
W = width of the enclosure, m
x,y,z = Cartesian coordinates, m
α = thermal diffusivity, $k/\rho c$, m^2/s
β = isobaric volumetric coefficient of expansion
υ = kinematic viscosity, kg/m^3
ρ = density, kg/m^3

Subscripts
c = cold wall
f = average fluid temperature
h = heated section
L_1 = based on the height of the heated section
y = based on the local height measured from the bottom of the enclosure to the midheight of a given heater

Introduction

WITH the continuing development of electronic technology, the effective cooling of microelectronic components has become increasingly important. Natural convection plays an important role, since it provides simple, low-cost, reliable, maintenance-free, and electromagnetic interference-free cooling.[1] Therefore, research work on natural convection in fluid-filled enclosures is of current interest.[2] In some cases, the electronic components can be modeled as whole flat plates or as discrete flat arrays on a vertical wall. However, in some situations, the actual cooling configuration is of higher geometrical complexity, in which case the electronic components can only be considered as arrays protruding from a vertical wall.

A number of investigators have reported results on buoyancy-driven convection due to flush-mounted heat sources. Chu et al.[3] experimentally and numerically studied natural convection due to a heated strip located on a side wall of a rectangular enclosure. They investigated the effect of heater size heater location, and the aspect ratio of the enclosure on the flow pattern and heat transfer. Sparrow and Faghri[4] numerically investigated the problem of two in-line, flush-mounted isothermal heaters on a vertical plate undergoing natural convection in air. Jaluria[5,6] numerically solved the similar problem for multiple heaters and then numerically as well as experimentally investigated two-line sources.[6] Turner and Flack[7] experimentally investigated natural convection in an air-filled enclosure with an isothermally heated vertical wall. They studied the effects of heater location and size on the rate of heat transfer. Park and Bergles[8] experimentally studied free convection from both in-line and staggered arrays of heaters with variable spacing between heaters. They also

Received Feb. 2, 1989; revision received Aug. 4, 1989.

*Lecturer, Department of Thermal Engineering.
†Assistant Professor, Department of Mechanical and Aerospace Engineering.
‡Professor and Head, Department of Mechanical and Aerospace Engineering. Senior Member AIAA.

reported results for the case of protruding surfaces with a protrusion height of 1.1 mm. Recently, Keyhani et al.[9] performed experiments of natural convection heat transfer in a tall vertical cavity (aspect ratio = 16.5), with one isothermally cooled vertical wall and 11 alternatively unheated and flush-heated sections of equal height on the opposite vertical wall. The flow visualization pictures revealed the existence of primary, secondary, and tertiary flows. Another paper by Keyhani et al.[10] extended the previous work with an experimental and numerical study of the problem in an enclosure with an aspect ratio of 4.5 and three heated sections. They indicated that, at a given modified Rayleigh number, the Nusselt number for a dielectric fluid ($Pr = 25$) was nearly the same as that of ethylene glycol ($Pr = 166$). Moreover, the flow patterns for the two fluids were nearly identical at a given modified Rayleigh number. Thus, the results of experimental research with ethylene glycol are applicable to immersion cooling with dielectric fluids.

Very few efforts have been made for cases of complex geometry. Ortega and Moffat[11,12] reported experimental results on naturally induced convection from an array of cubical elements that were deployed in an in-line array on one vertical wall. They indicated that the heat transfer was driven primarily by globally induced channel flow, rather than by the local buoyancy mechanism. Shakerin and Loehrke[13] presented a numerical analysis on two-dimensional natural convection flow over single and repeated roughness elements attached to the heated wall of an enclosure. Their results indicate that the average Nusselt number for a vertical wall in the presence of roughness is only slightly higher than that for a smooth wall. Kuhn and Oosthuizen[14] conducted a numerical study of three-dimensional transient natural convective flow in a rectangular enclosure with localized heating. They point out that the three-dimensional flow increased the local heat transfer coefficient at the edge of the element and caused the average Nusselt number to be higher than that in the corresponding two-dimensional flow at low Rayleigh numbers (less then 10^5). Kelleher et al.[15] presented experimental results (part I) and Lee et al.[16] a numerical analysis (part II) for natural convection in a water-filled rectangular enclosure with one small heater protruding from a vertical wall. Experiments were conducted with the heater at three different locations: near the top, in the middle, and near the bottom of the wall. The results indicate that for a given Rayleigh number, the local Nusselt number decreased as the heater was raised in the enclosure. The numerical work indicated good agreement with the results of experiments in the higher Rayleigh number range covered by the experiments; the numerically predicted values were consistently higher than measured values in the lower Rayleigh number range.

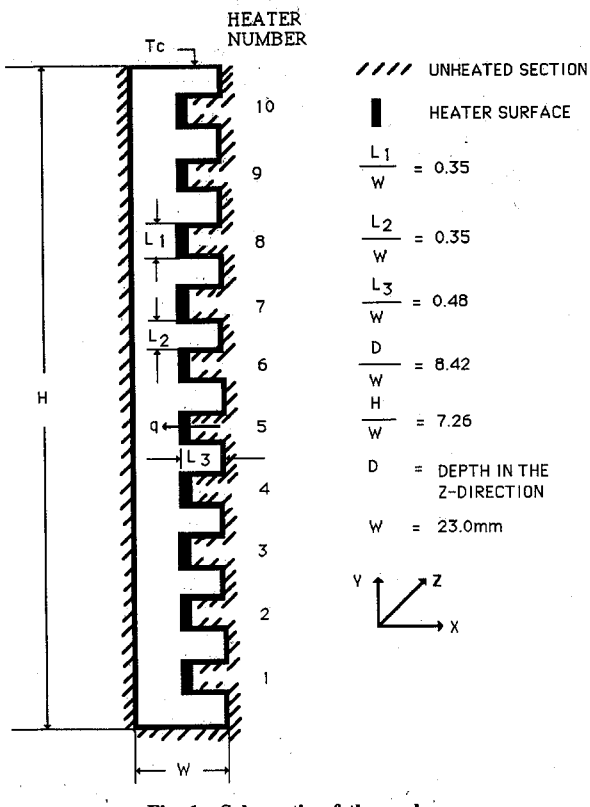

Fig. 1 Schematic of the enclosure.

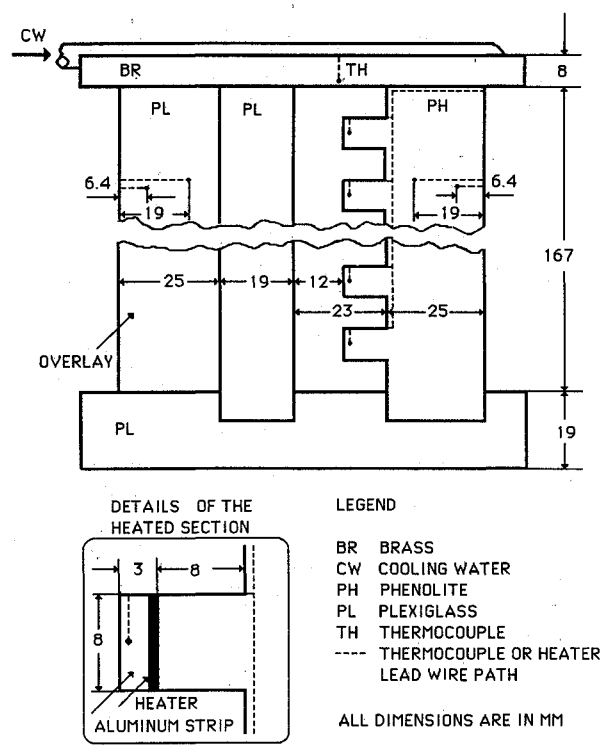

Fig. 2 Construction details of the experimental apparatus.

A numerical study of three-dimensional convective cooling of an array of heated protrusions in an enclosure filled with a dielectric fluid was reported by Liu et al.[17] in which a 3×3 array of protruding chips mounted on one vertical wall were heated. Results indicated that the maximum temperature always happens alternately among the three top chips as time proceeds in a rather regular fashion. It was also seen that there was little interference among the chips, especially for the lower two rows. The heat transfer characteristics were strongly affected by the stratified temperature field from the chip.

From the preceding review of pertinent literature, it is evident that the understanding of natural convection in a fluid-filled enclosure with multiple protruding heaters is limited. The flow structure as well as heat transfer characteristics have not been thoroughly explored. Therefore, the objectives of the present work are to investigate experimentally the natural convection heat transfer in a rectangular cavity with protruding heaters, to study the flow structure and heat transfer characteristics under different levels of power dissipation, and to determine useful heat transfer correlations.

Experimental Apparatus and Procedure

The experimental apparatus consisted of a liquid-filled rectangular enclosure with 10 protruding heaters uniformly spaced on one of the vertical walls. The top surface of the enclosure was a heat sink held at constant temperature. All of the other surfaces, except the heater locations, were unheated. The enclosure was 16.7 cm in vertical height, 2.3 cm in width, and 19.6 cm in depth (horizontal z direction of the heaters). The 10 heaters measured 1.11 cm in horizontal (x direction)

protuberance dimension, 0.8 cm in vertical height (y direction), and the same depth as that of the enclosure. The gap between heaters was equal to the vertical height of the heaters and measured 0.8 cm. All of the geometrical details are shown in Figs. 1 and 2. The vertical wall with heated protrusions was made of phenolite plate and was 2.54 cm thick. This plate was milled to form alternating, equally sized rectangular protrusions. A thermal strip heater was attached on the vertical surface of each protrusion, and this heater was in turn covered by a thin (3-mm-thick) aluminum strip.

The top plate of the enclosure was made of 8-cm-thick brass to ensure a suitably high rate of conductive heat transfer. Machined into this brass plate was a groove to contain a section of brass tube soldered continuously to the plate. Cooling water from a constant-temperature circulating bath was run through this tube to maintain the plate at a constant temperature. The circulator maintained water temperature within ± 0.1°C. Included with the top plate was a rubber O-ring used to seal the enclosure and reduce the conduction between top plate and vertical walls. The top plate and O-ring were secured with threaded rods and nuts, which were screwed into the enclosure base.

The two side walls, the wall opposite the heater wall, and the bottom plate were all made of Plexiglas, with thicknesses of 0.48, 1.9, and 1.9 cm, respectively. Since the vertical sidewall opposing the heated surfaces was desired to be clear for viewing, a Plexiglas plate was placed behind this wall to reduce conduction losses. This plate was present during collection of heat transfer data and was removed for flow visualization experiments.

Sixteen copper-constantan thermocouples were placed on the vertical surfaces of the 10 protrusions to measure the temperatures of all of the heaters. One thermocouple was located in the middle of each heater, and the remaining six were placed one on each of the two ends of heaters 1, 6, and 10. It should be noted that, as shown in Fig. 1, the heater numbering starts from the bottom. Thermocouples were also placed at different depths in the vertical and bottom surfaces to permit calculation of the conduction heat losses through surfaces. Six thermocouples were located equidistantly along the top plate to measure the cold temperature and to assure that the top plate was indeed at a constant temperature. All power wires and thermocouple leads were taken out through three channels milled in the phenolite plate and were connected to a power panel and a digital temperature data acquisition system, respectively.

Power was supplied through a power panel that consisted of a voltage stabilizer, a stepdown transformer, and three manually controlled voltage regulators. Each regulator was used to supply power to one of three circuits. Heaters 1-3, 4-6, and 7-10 formed three separate circuits. Voltage information for each heater circuit was fed to an HP 3054A data acquisition system coupled with an HP 9817H computer for data collection and analysis.

Distilled water and glycol were used as working fluids. In each case, the experiment started using a power setting of 1 W to each heater. The power input to each heater in the subsequent runs was increased by 1 W for each run, until a local maximum temperature of 80°C was obtained. After the steady state was reached for each run, all of the temperatures, voltages, and current readings to each heater circuit were collected.

In order to observe the flow pattern, visualization experiments were performed under several power input conditions. Aluminum powder (5-20 μ in size) was used as the tracer particle with glycol as the convective medium. The aluminum particles were illuminated by suitable lighting to obtain photographs.

Data Reduction

The thermophysical properties of both glycol and distilled water were evaluated at the average temperature of a given heater surface and the top plate, that is,

$$T_f = [(T_h + T_c)/2] \tag{1}$$

where T_h is the local temperature at the midheight of a given heater surface, and T_c is the temperature of top sink surface. This simple arithmetic mean temperature T_f was also emphasized in the reports of Kelleher et al.[15] and Lee et al.[16] For each heater, T_h was different, therefore, there were 10 different T_f for the heaters. The local convective heat transfer coefficient h is defined by

$$h = q/(T_h - T_c) \tag{2}$$

where $(T_h - T_c)$ is the temperature difference between heater surface and the cold plate.

The heat flux by convection is calculated with

$$q = (Q - Q_L - Q_{sc})/A_h \tag{3}$$

where Q is the power input to each heater. Q_L is the heat loss per heater to the environment by conduction through the back of the vertical wall on which heaters are mounted, the opposite wall, two end walls, and the bottom plate. The heat loss through the vertical wall with heaters does not enter the enclosure. The heat loss from the opposite wall is 4-7% and 1.7-3.6% for glycol and water, respectively. The heat loss through the bottom is 1.8-3.6% and 0.7-1.9% for glycol and water, respectively. The heat loss through the two end side walls is below 1.0% for both working liquids. Q_{sc} is the substrate conduction heat transfer, convected from the unheated phenolite surface. The ratio of $Q_{sc}/(Q - Q_L)$ depends on power input and working fluid. Using a numerical analysis to determine Q_{sc}, this ratio has been found to be about 8-18% for experiments conducted with glycol, and less than 2% for tests with water. The lower value of this ratio corresponds to the highest power setting per heater; the upper value is for the lowest power setting. In Eq. (3), A_h is the total exposed surface area of the thin (3-mm-thickness) aluminum plate on the top of each heater.

The Nusselt number and modified Rayleigh number are defined as

$$Nu = h\,[\text{length scale}]/k \tag{4}$$

$$Ra^* = g\beta q\,[\text{length scale}]^4/k\nu\alpha \tag{5}$$

Two length scales of local height y (Nu_y, Ra_y^*) and the height of the heated section L_1(Nu_{L_1},$Ra_{L_1}^*$) are used in the presentation of the results.

Uncertainty Analysis

In experiments, the thermocouple outputs were measured to $\pm 0.1\ \mu V$, which yielded 0.0025°C of sensitivity. The accuracy of temperature measurement is estimated as ± 0.15°C. This estimate includes the errors introduced by reference junction compensation (± 0.01°C), temperature difference along terminals, thermal offset, voltage conversion error, and DVM accuracy. It should be noted that this estimate has been verified by comparison with a precision thermometer calibrated by the National Bureau of Standards. The voltage input to each heater circuit was measured with a sensitivity of ± 0.1%. Comparison between the original resistance of each heater circuit accurately measured before experiment and the average resistance after being heated and cooled to room temperature indicated that the maximum uncertainty for resistance could be conservatively considered as ± 2%. The uncertainty of length scale for the heaters was ± 0.25 mm. The thermophysical properties of the glycol and distilled water were estimated with an uncertainty of ± 2%, which was based on the observed variations in the reported values in the literature.

Uncertainty analysis using the standard Kline-McClintock approach indicates that the uncertainty of the Nusselt number and Rayleigh number varies with power input. A lower power

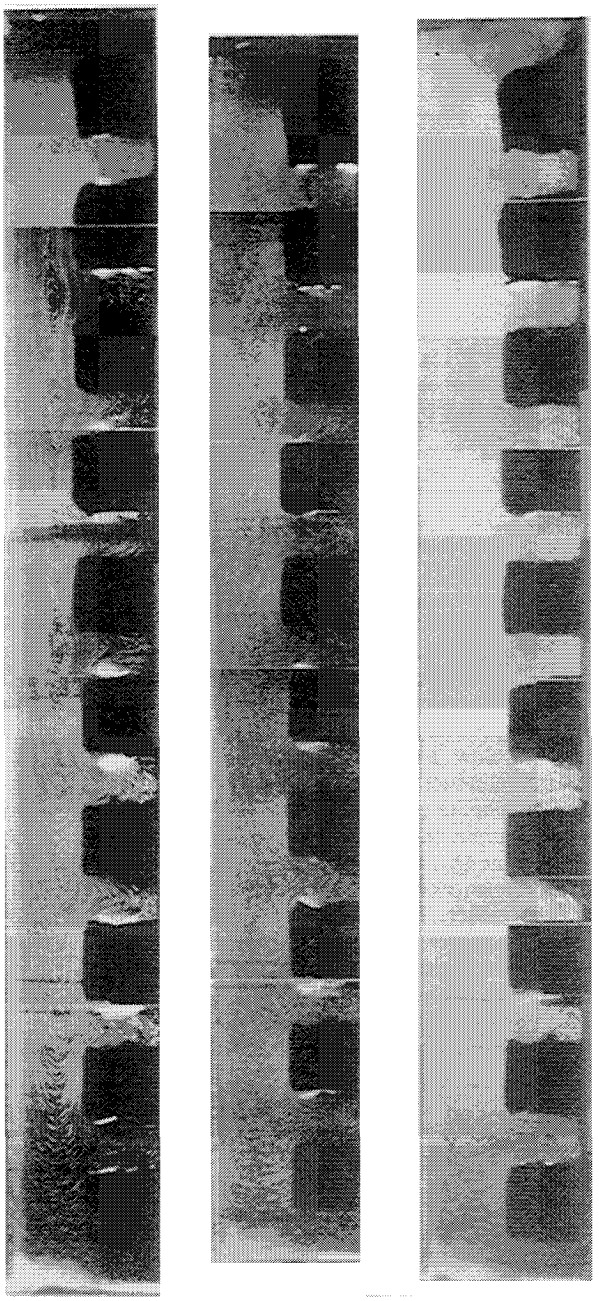

Fig. 3 Flow structure within the enclosure.

input results in a higher uncertainty because of the higher fraction of heat losses by conduction. By calculation, the uncertainties of Nu_y and Ra_y^* were estimated as 5.2–6.4% and 6.8–8.3%, respectively, for glycol, and 5–6% and 6–8.6%, respectively, for distilled water.

Results and Discussion

Flow Visualization

Figure 3 represents typical flow structures within the whole enclosure at the power inputs of 2, 6, and 8 W per heater. There is a very strong primary flow that travels up along the heater surfaces, enters the gap between heaters, and eventually descends along the opposing unheated vertical surface. Evidently, the primary flow provides the main contribution to the heat transfer. Between the primary flows (upward on the right and downward on the left), there exists a core flow composed of secondary flow cells. This core occupies almost the entire height of the enclosure. At the bottom of the core, the secondary flow is not strong. The first whole secondary cell in the core appears at a vertical location between heater 3 and heater 4. Above heater 3 and corresponding to the position of each unheated gap, one small secondary cell can be found. The core flow ends at the middle of heater 10.

In the gap between the heated sections, a recirculating cell moving in the clockwise direction, opposite to that of the primary flow, is observed. At the bottom of the enclosure the fluid moves slowly in the primary flow and can enter the gap very deeply; therefore, the recirculating cell is very small. However, at the top portion of the enclosure, the primary flow velocity is higher and cannot enter the gap as deeply as it does at the bottom. Consequently, the recirculating cell appears much larger in the gap near the top. This can be seen more clearly in the photograph with 2 W per heater.

With an increase in the power input, the flow in the core becomes wider and gradually transforms to unsteady flow, which can be seen in the pictures with 8 and 10 W per heater, even though the primary flow is still laminar. As the heat transfer rate increases, the fluid velocity also increases, and the depth to which the primary flow enters the horizontal gap decreases. Moreover, because of the higher velocity in primary flow, the shear stress caused by primary flow is gradually

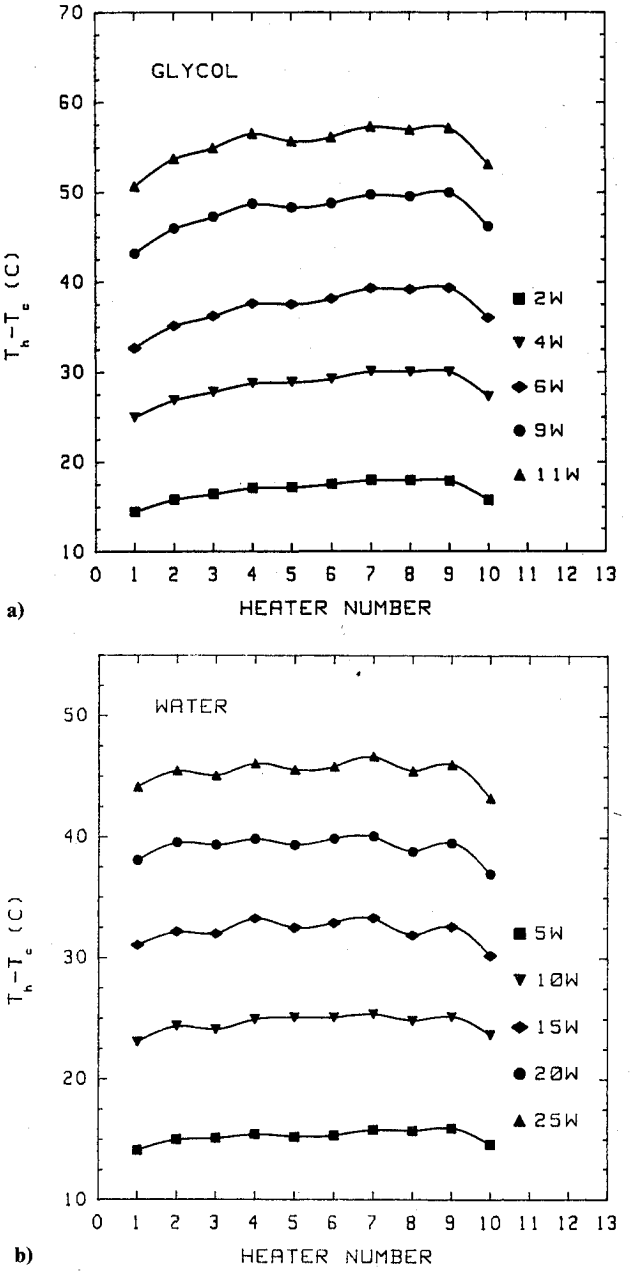

Fig. 4 Excess temperature, $(T_h - T_c)$, of the heaters; a) glycol data and b) water data.

increased, and thus the secondary flow gradually changes to unsteady flow.

Temperature Distribution

The excess temperature of the heated sections, $(T_h - T_c)$, for working fluids of glycol and water are presented in Figs. 4a and 4b, respectively. The glycol data, Fig. 4a, show that the bottom heater ($N = 1$) has the lowest excess temperature, whereas the location of the maximum of $(T_h - T_c)$ fluctuates between $N = 7$, 8, and 9. It should be noted that the variation of the $(T_h - T_c)$ for heaters 7, 8, and 9 from their mean value is less than 0.5%. Thus, one can state that the region covered by $N = 7$, 8, and 9 is the location of maximum excess temperature. Despite the complexity of the present problem, it is important to note that the data in Fig. 4a indicate that the $(T_h - T_c)$ for heaters 2-9 (at a given power input) can be approximated with an average value to within ± 3%.

The modified Raleigh number ranges for the glycol and water data are $2 \times 10^4 < Ra^*_{L_1} < 7 \times 10^5$ and $4 \times 10^4 < Ra^*_{L_1} < 3.5 \times 10^6$, respectively. The discussion of the water temperature data of Fig. 4b, with the exception of the location of the minimum excess temperature, is similar to that presented for the glycol results. The minimum excess temperature for runs with $Ra^*_{L_1} < 7 \times 10^5$ (corresponding to Q< 10 W) is observed to occur at heater 1, which is the same result as that for the glycol data. However, for $Ra^*_{L_1} > 7 \times 10^5$ (higher values than the glycol range), the minimum $(T_h - T_c)$ occurs at heater 10. The agreement between the observed location of minimum $(T_h - T_c)$ for water and glycol data for $Ra^*_{L_1} < 7 \times 10^5$ indicates that the Prandtl number difference of the two liquids is not a strong factor in the change of the location of minimum temperature difference (or excess temperature) when $Ra^*_{L_1} > 7 \times 10^5$.

In order to show the effect of stratification, the temperature differences $(T_h - T_{core})$ obtained with glycol as the working fluid are presented in Fig. 5 for several power inputs. The core temperatures were measured with a thermocouple probe at each heater elevation at the midgap distance between the protrusion and the opposing wall. The $(T_h - T_{core})$ values do not exhibit a smooth variation between the 10 heaters. However, with the exception of minor fluctuations in the interim, the general trend is an increase of $(T_h - T_{core})$ with increasing N over the range from $N = 1$ to $N = 9$. The $(T_h - T_{core})$ of the top heater drops sharply, due to the proximity of heater 10 to the top isothermal surface and the rather high core temperature at that location.

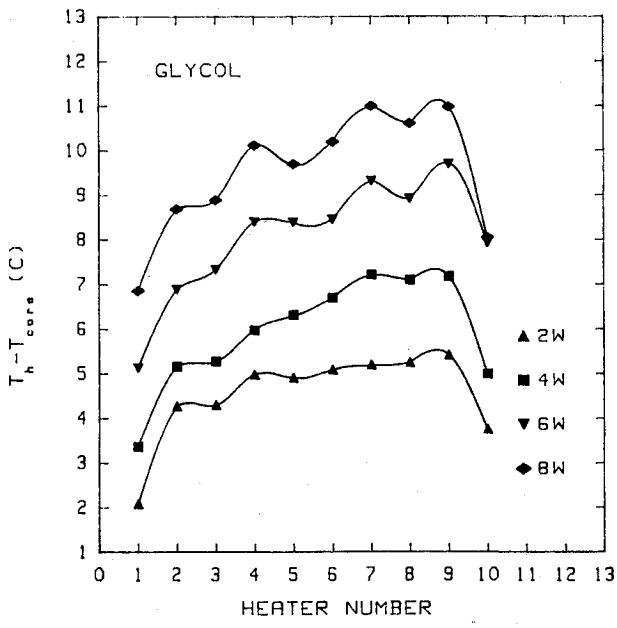

Fig. 5 $(T_h - T_{core})$ distribution – glycol data.

Heat Transfer

The variations of the Nusselt number as a function of modified Rayleigh number based on the height of the heated section, $Ra^*_{L_1}$, for glycol and water as working fluids are shown in Fig. 6. For a given modified Rayleigh number, the lowest Nusselt number usually occurs at heaters 7, 8, and 9. With increases up to heater 7. Generally, the highest Nusselt number is for heater 1, with the exception of the high Rayleigh number data.

In the case of glycol as the working fluid, the Nusselt numbers for heaters 10 and 2 are almost equal and lower than that of heater 1. With distilled water, the Nusselt number at heater 10 is slightly lower than that of heater 1 for $Ra^*_{L_1} < 7 \times 10^5$. As the modified Rayleigh number is increased beyond 7×10^5, heater 10 attains the highest heat transfer coefficient. This situation implies the existence of a transition in flow structure near the top heater.

Kelleher et al.[15] noticed that the Nusselt number tends to decrease as the local height position of the single protruding heater within the enclosure is increased. In this case, only one protruding heater was employed. Their flow was basically dual-celled: there was a buoyancy driven lower cell in which the fluid motion was due to the viscous drag from the upper cell. They found that the location of the cell separation shear layer is dependent on the position of the heater within the enclosure and is always near the lower surface of the heater. When the heater is located near the bottom of the enclosure, the shear driven lower cell is very small, which results in a rather lower amount of drag force on the upper cell; therefore, the liquid velocity across the heater is high. As the heater is moved to the middle of the enclosure, the shear driven cell is much larger than before. Of course, it requires larger drag from the upper cell to drive the lower cell. When the heater is mounted near the top, the energy required to drive the large lower cell is at a maximum and the upper velocity is at a minimum; therefore, the heat transfer coefficient is at a minimum.

In the present work there were 10 heaters operating simultaneously. Thus, shear driven cells exist in the gaps between heaters only. As liquid rises along the heated surfaces, the temperature of the liquid near the heaters is increasing, which in turn results in a higher heater surface temperature. This effect tends to decrease the local heat transfer coefficient, whose definition is based on the temperature differences between the heater and the sink surface. On the other hand, high temperature of the liquid results in a stronger buoyant force

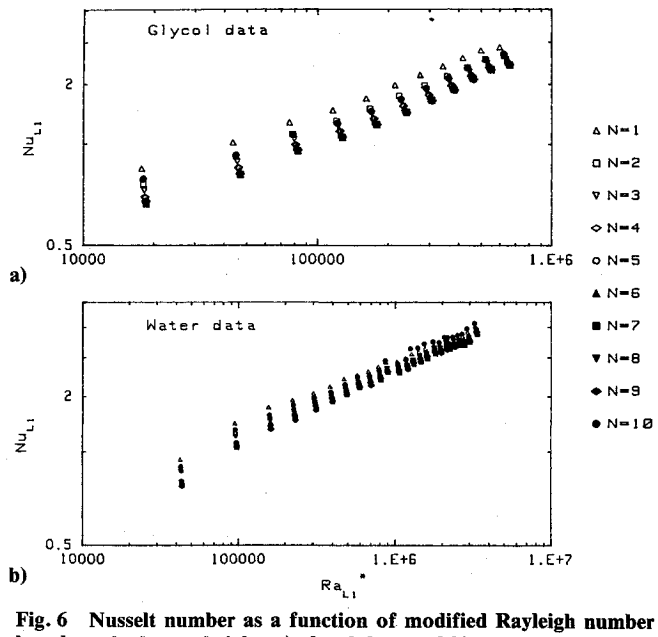

Fig. 6 Nusselt number as a function of modified Rayleigh number based on the heater height; a) glycol data and b) water data.

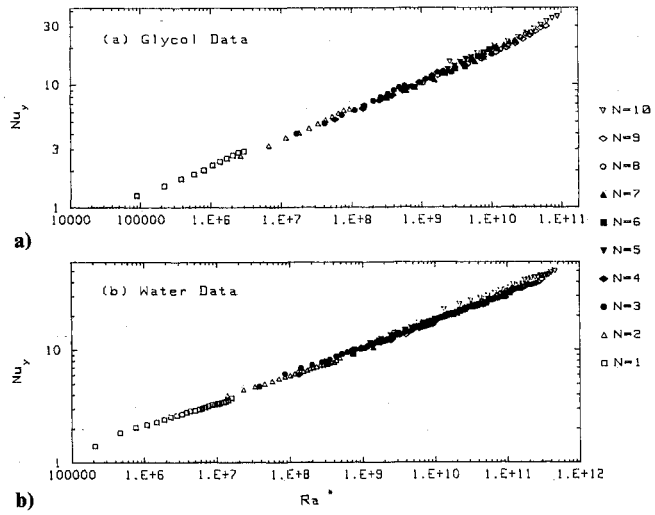

Fig. 7 Local Nusselt number as a function of modified Rayleigh number based on local height; a) glycol data and b) water data.

and a relatively higher velocity of the liquid near the heater surface. This, in turn, tends to improve the local heat transfer coefficient. The net effect of these opposing factors determines the local heat transfer coefficient. It should be noted that heater 10 experiences extremes of these effects more than any other heater, as well as the fact that it is closest to the sink surface. Thus, it is very difficult to predict how these opposing factors and the proximity to the sink surface will affect the local heat transfer coefficient.

Following the aluminum particles traveling along the heater surface, liquid (glycol) velocity near the surface of each heater was measured with a stop watch and scale. At a power setting of 8 W to each heater, the local velocity increases from 1.6 mm/s at $N = 1$ to 4.0 mm/s at $N = 5$, and finally to 8.0 mm/s at $N = 10$. These measurements are not very accurate, but the trend is evident.

The presentation of the Nu_{L_1} vs $Ra^*_{L_1}$ in Fig. 6 suggests that, for a given fluid 10 different correlations (one for each heater) are needed in order to report the heat transfer data. However, by representation of the data based on the length scale of local heights y, it will be shown that this is not the case. Local Nusselt numbers Nu_y as a function of local modified Rayleigh numbers Ra_y^* are presented in Fig. 7. It is interesting to note that the log-log plot of Nu_y vs Ra_y^* for all heaters forms a distinct straight line for each of the two working fluids. Thus, for each fluid, a single correlation can represent the heat transfer coefficients for all of the heaters.

By linear regression analysis of the experimental data of the present study, heat transfer correlations relating the Nusselt number to the modified Rayleigh number, based on the heater local height, have been obtained. The correlation for glycol is

$$Nu_y = 0.0796\ (Ra_y^*)^{0.237} \tag{6}$$

The ranges of Ra_y^* and Pr for this expression are 8.7×10^4 to 8.7×10^{10} and 57 to 141, respectively. The average and maximum deviations from the data are 3.2% and 8.7%, respectively. The correlation for the water data is given by

$$Nu_y = 0.0678\ (Ra_y^*)^{0.243} \tag{7}$$

for the Ra_y^* and Pr ranges of 1.06×10^5 to 9.46×10^{10} and 3.3 to 6.2, respectively. The average and maximum deviations from the data are 3.3% and 7.3%, respectively. The utility of Eqs. (6) and (7) is restricted to the enclosures with geometric parameters, similar to those given in Fig. 1. The determination of the effect of the geometric parameters on the heat transfer coefficient is the main objective of our ongoing work, which will be reported in a timely manner.

Carmona and Keyhani[18] experimentally investigated the cavity width effect on immersion cooling due to five discrete flush heaters on one vertical wall of an enclosure cooled from the top. Even though the number and dimensions of the heaters were different from those of the present work, some comparison still can be made. They reported a heat transfer correlation for glycol as

$$Nu_y = 0.437\ (H/W)^{-0.416}\ Ra_y^{*0.227} \tag{8}$$

At $H/W = 7.26$, which is the same as that of the present work, this correlation becomes

$$Nu_y = 0.1916\ Ra_y^{*0.227} \tag{9}$$

The preceding correlation can be compared with the correlation for glycol from the present work. Equation (9) indicates that the flush-heaters case will result in higher local heat transfer coefficients. For example, at $Ra_y^* = 10^{10}$, the flush case [Eq. (9)] predicts a local Nusselt number of $Nu_y = 35.68$, whereas the present correlation for the protruded heaters case [Eq. (6)] yields a local Nusselt number of $Nu_y = 18.66$. Thus, it is evident that the protruded heated case results in lower heat transfer coefficients in cavity flow.

Conclusions

An experimental study of natural convection heat transfer in a rectangular enclosure with 10 identical and uniformly spaced protruding heaters has been carried out to investigate the heat transfer performance and flow patterns. Distilled water and glycol were used as working fluids. Photographs of the flow patterns as well as heat transfer correlations are presented. From the experimental results the following conclusions can be drawn:

1) The primary flow along the wall within the enclosure is very strong, and this flow is the main contributor to the heat transfer.

2) There is a narrow and long core flow, composed of secondary flow cells within the primary flow cell in which temperature is stratified. There are also secondary flow cells in the gaps between the protrusions.

3) The bottom heater, except for high Rayleigh number data, has the highest local heat transfer coefficient. The local heat transfer coefficients at heaters 7, 8, and 9 are nearly the same and have the lowest values. With increases of local height, the local heat transfer coefficient decreases up to heater 7. However, at heater 10 the heat transfer coefficient increases and is much larger than those for heaters 7, 8, and 9.

4) The log-log plot of Nu_y vs Ra_y^* for all 10 heaters formed distinct straight lines for each of the two working fluids.

The present work is considered to be a basis for further study. The influence of geometrical dimensions on heat transfer and flow structure, natural convection with multiple three-dimensional protrusions, etc., are topics to be considered in future studies.

References

[1]Johnson, C. E., "Evaluation of Correlation for Natural Convection Cooling of Electronic Equipment," *Heat Transfer in Electronic Equipment—1986*, American Society of Mechanical Engineers, HTD-Vol. 57, 1986, pp. 103–111.

[2]Yang, K. T., "Natural Convection in Enclosures," *Handbook of Single Phase Convection Heat Transfer*, edited by W. Aung, S. Kakac, and R. K. Shah, Wiley, New York, 1987, pp. 13.1–13.51.

[3]Chu, H. H-S., Churchill, S. W., and Patterson, C. V. S., "The Effect of Heaters Size, Location, Aspect Ratio, and Boundary Conditions on Two Dimensional, Laminar, Natural Convection in Rectangular Channels," *ASME Journal of Heat Transfer*, Vol. 98, No. 1, 1976, pp. 194–201.

[4]Sparrow, E. M., and Faghri, M., "Natural Convection Heat Transfer from the Upper Plates," *ASME Journal of Heat Transfer*, Vol. 102, No. 3, 1980, pp. 623–629.

[5]Jaluria, Y., "Buoyancy-Induced Flow Due to Isolated Thermal Sources on a Vertical Surface," *ASME Journal of Heat Transfer*, Vol. 104, No. 1, 1982, pp. 223–227.

[6]Jaluria, Y., "Natural Convection Flow Due to Line Thermal Sources on a Vertical Adiabatic Surface," *Proceedings of the 7th International Heat Transfer Conference*, Vol. 2, Hemisphere, New York, 1982, pp. 147-152.

[7]Turner, B. L., and Flack, R. D., "The Experimental Measurement of Natural Convection Heat Transfer in Rectangular Enclosures with Concentrated Energy Sources," *ASME Journal of Heat Transfer*, Vol. 102, No. 2, 1980, pp. 236-241.

[8]Park, K-A., and Bergles, A. E., "Natural Convection Heat Transfer Characteristics of Simulated Microelectronic Chips," *ASME Journal of Heat Transfer*, Vol. 109, 1987, pp. 90-96.

[9]Keyhani, M., Prasad, V., and Cox, R., "An Experimental Study of Natural Convection in a Vertical Cavity with Discrete Heat Sources," *ASME Journal of Heat Transfer,* Vol. 110, 1988, pp. 616-624.

[10]Keyhani, M., Prasad, V., Shen, R., and Wong, T-T., "Free Convection Heat Transfer from Discrete Heat Source in a Vertical Cavity," *Natural and Mixed Convection in Electronic Equipment Cooling*, edited by R. A. Wirtz, American Society of Mechanical Engineers, HTD-Vol. 100, 1988, pp. 13-24.

[11]Ortega, A., and Moffat, R. J., "Heat Transfer From a Array of Simulated Electronic Componets: Experimental Results for Free Convection With and Without a Shrouding Wall," *Heat Transfer in Electronic Equipment—1985,* American Society of Mechanical Engineers, HTD-Vol. 48, 1985, pp. 5-15.

[12]Moffat, R. J., and Ortega, A., "Buoyancy Induced Forced Convection," *Heat Transfer in Electronic Equipment—1986*, American Society of Mechanical Engineers, HTD-Vol. 57, 1986, pp. 135-144.

[13]Shakerin, S., and Loehrke, R., "A Numerical Study of Natural Convection Over Discrete Roughness Elements on a Vertical Heated Wall of an Enclosure," *Proceedings of 2nd ASME/JSME Thermal Engineering Joint Conference*, Honolulu, HI, Vol. 2, 1987, pp. 261-267.

[14]Kuhn, D., and Oosthuizen, P. H., "Three-Dimensional Transient Natural Convective Flow in a Rectangular Enclosure with Localized Heating," *Natural Convection in Enclosures—1986*, American Society of Mechanical Engineers, HTD-Vol. 63, 1986, pp. 55-62.

[15]Kelleher, M. D., Knock, R. H., and Yang, K. T., "Laminar Natural Convection in a Rectangular Enclosure Due to a Heated Protrusion on One Vertical Wall Part I: Experimental Investigation," *Proceedings of 2nd ASME/JSME Thermal Engineering Joint Conference*, Honolulu, HI, Vol. 2, 1987, pp. 169-177.

[16]Lee, J. J., Liu, V. K., Yang, K. T., and Kelleher, M. D., "Laminar Natural Convection in a Rectangular Enclosure Due to a Heated Protrusion on One Vertical Wall Part II: Numerical Simulation," *Proceedings of 2nd ASME/JSME Thermal Engineering Joint Conference*, Honolulu, HI, Vol. 2, 1987, pp. 179-185.

[17]Liu, K. V., Yang, K. T., and Kelleher, M. D., "Three-Dimensional Natural Convection Cooling of an Array of Heated Protrusions in an Enclosure Filled with a Dielectric Fluid," *Proceedings of International Symposium on Cooling Technology for Electronic Equipment,* Honolulu, HI, 1987, pp. 486-497.

[18]Carmona, R., and Keyhani, M., "The Cavity Width Effect on Immersion Cooling Due to Discrete Flush-Heaters on One Vertical Wall of an Enclosure Cooled from the Top," *ASME Journal of Electronic Packaging,* Vol. 111, No. 4, 1989, pp. 268-276.